Computational study on photo- and thermo-reactions between tetra-*tert*-butyl-substituted cyclobutadiene and tetrahedrane

Masato Sumita,[*,a] Kazuya Saito,[*,b] Yoshitaka Tateyama[a]

E-mail: M.S., SUMITA.Masato@nims.go.jp; K. S., kazuya@chem.tsukuba.ac.jp

[a]*WPI International Centre for Materials Nanoarchitectonics (MANA), National Institute for Materials Science (NIMS), 1-1 Namiki, Tsukuba, Ibaraki 305-0044, Japan*

[b]*Department of Chemistry, Graduate School of Pure and Applied Sciences, University of Tsukuba, 1-1-1 Tennodai, Tsukuba, Ibaraki 305-8571, Japan*

Abstract

We have investigated the photo-chemical reaction from tetra-*tert*-butylcyclobutadiene (TB-CBD) to tetra-*tert*-butyltetrahedrane (TB-THD) and its reverse thermo-chemical reaction processes in the ground state by using CASSCF and MRMP2 computational methods. According to our results, the initial step of the photochemical reaction is the HOMO-LUMO single-electron excitation (1^1B_1 state) and the arrangement from TB-CBD to TB-THD occurs via the HOMO-LUMO double electron excited state (2^1A_1 state). After the transition from the 1^1B_1 to the 2^1A_1 state, most TB-CBD molecules show only photo-physical property without any reactions because the final point of the minimum-energy-path (MEP) calculation at the MRMP2//CASSCF level is the S_1/S_0 conical intersection (ionic like structure), which results in turning back to TB-CBD in the S_0 state. However, on the way to the final point of the MEP, it is possible for some TB-CBD to transit at another S_1/S_0 conical intersection (tetra radical like structure), which is related to the photoreaction from TB-CBD to TB-THD. On the other hand, two routes from TB-THD to TB-CBD were found in the S_0 state. One is the route via bicyclodiradical transition state. The other is the ionic transition state. In both reaction

paths, only one TS is there in contrast to the plural step reaction suggested previously.

1.Introduction

Chemical bond between carbon atoms can be formed in surprisingly strained situations. Tetrahedrane (THD) is one of the most strained organic molecules [1,2]. Considering the sp^3 hybridized orbital, the ideal bond angle is 109.5°. However, a carbon atom of THD should tolerate an extremely sharp angle (60°) in spite of its sp^3 like bonding style. Its exotic shape has fascinated many experimental and theoretical chemists. Not only the object of art but a practical application as some reagent is expected because of its tremendous basicity, probably induced by its strained structure [3]. We think that THD species have potentials to become a part of functional or photo-induced functional molecules because of its peculiar shape and photo/thermo-reactivity. Therefore, the understanding its fundamental reactivity and photo-induced processes is important.

In spite of experimental chemist's efforts, unfortunately, the parent (un-substituted) THD has not been isolated yet. Our computational results [4] predicted that THD could be isolated only at very low temperatures because one or two bonds of THD will be broken easily with the energy barriers less than 17 kJ mol^{-1}. In order to stabilize the

tetrahedral structure, four bulky substituents seem to be needed. Indeed, some derivatives with four bulky substituents had been isolated [1,2,5,6]. The substituents utilized so far are σ-donating such as *tert*-butyl and trimethylsilyl [1,2,5]. Therefore, it is considered that the steric repulsion between the bulky substituents makes tetrahedral shape stabilized. This stabilization effect is called "corset-effect" [2,5,6]. However, the steric repulsion between trimethylsilyl groups of tetratrimethylsilyltetrahedrane (abbreviated as TmS-THD hereafter) is considered to be weaker than that of *tert*-butyl group of tetra-*tert*-butyltetrahedrane (TB-THD). Furthermore, the recent successful product has a π–σ conjugation system [6]. Therefore, the tetrahedral shape seems to be stabilized by not only steric effect but also electronic effect.

The first thermally stable THD is TB-THD, which is synthesized from tetra-*tert*-butylecyclopentadienone as colorless crystals [2,7]. Upon heating up to 130 °C, the colorless solution of TB-THD in 1,1,3,3,5,5-hexakis(trideuteriomethyl)-l,3,5-trisilacyclohexane changes into yellowish orange liquid, which is attributed to the absorption at 425 nm of tetra-*tert*-butylcyclobutadiene (TB-CBD). This fact indicates that TB-THD thermally isomerizes to TB-CBD. Interestingly, TB-THD is regenerated

by irradiating TB-CBD with the light whose wavelength is > 300 nm in a solution at room temperature or in argon at 10 K (criss-cross reaction: Scheme 1) [2,7].

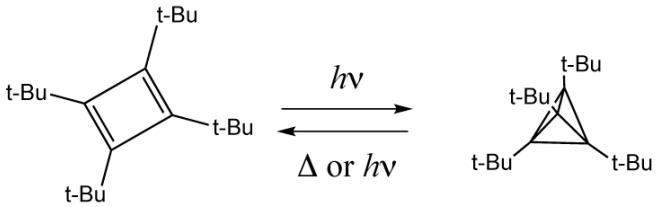

Scheme 1

Other CBD derivatives exhibit similar photochemical reactions [2,5,7,8]. The wavelength of reactive light depends on derivatives (≥ 300 nm or 256 nm) [2,5,7,8]. The wavelength of reactive light is > 300 nm in the case of TB-CBD [2,7], whereas it is 256 nm for TmS-CBD [5]. Irradiation time for isomerization is longer than seven hours [5]. Furthermore, the analogous photoreaction from 1,2,3,4-tetra-*tert*-butylnaphthalene to 1,2,5,6-tetra-*tert*-butyle-3,4-benzo-3-tricyclohexene occurs by light whose absorption intensity is very weak [9]. This means that the criss-cross reaction [2,7] is hard to occur.

The rearrangement between CBD and THD is a symmetry-forbidden reaction since the occupied and unoccupied orbitals should be crossed during this rearrangement as seen in the orbital correlation diagram in Ref. [4]. Probably, this is one of the factors that make THD derivatives thermally stable and the CBD to THD rearrangement is

achieved only by light irradiation. Since the TB-CBD to TB-THD photoisomerization found in 1978 [7], however, not only this reaction process but also the responsible excited state for this reaction had not been elucidated yet. Probably, many difficulties (molecular size and computational resources, etc.) prevented theoreticians from exploring the potential energy surfaces (PESs) even though the many methodologies for excited states have been developed.

According to the orbital correlation diagram (in Ref. [4]), the HOMO to next LUMO double-electron excited state is the most plausible as the active state for the reaction from CBD to THD since the electron configuration of the excited state becomes that of the ground state of THD. However, its vertically excited state is energetically too high according to our preliminary calculation [10]. We predicted that the HOMO to LUMO double-electron excited state is alternatively responsible for this photoreaction on the basis of qualitative discussion. However, it seems to be not easy to achieve the photoreaction from the parent CBD to THD via the HOMO-LUMO double-electron excited state. In this paper, for more practical system, i.e., TB-CBD/TB-THD, we suggest the reaction processes through a computational method. Furthermore, we will

prove our qualitative prediction is reasonable.

The TB-THD to TB-CBD thermal reaction is predicted through the model calculation of the parent THD to CBD. According to the previous calculations [5, 11], it is assumed that the THD to CBD rearrangement occurs via the following plural-step reaction process (Scheme 2): First, by breaking of one bond of THD, exo-bicyclodiracial is produced. Second, the exo-bicyclodiradical converts to an endo-species. Finally, the endo-species isomerizes to CBD.

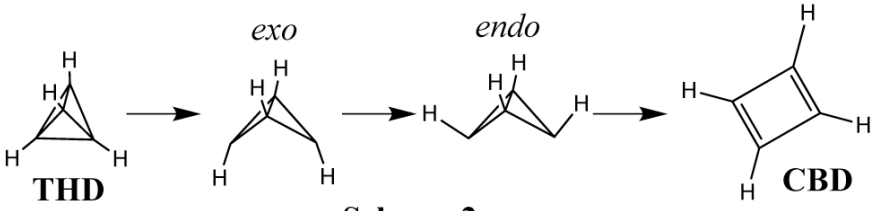

Scheme 2

Thermal reaction process in scheme 2 is based on the PES calculated by single-determinant based methods, i.e., HF, MP2, or MINDO/3 [5, 11]. Since crossing (degeneracy) between the occupied and unoccupied orbitals is expected in this rearrangement [4], multi-configuration based calculation [e.g., the complete active space self-consistent field (CASSCF) theory] is more suitable for the theoretical analysis of this system [12]. Moreover, it is suspicious to employ single-determinant based methods even for the equilibrium structures of TB-CBD and TB-THD. The

experimental results indicate that the TB-THD to TB-CBD rearrangement should be exothermic reaction [3,13]. However, even recent theoretical calculations at the density functional theory level do not reproduce this fact. According to the B3LYP/6-31G* calculation [3,14], indeed, TB-THD is more stable than TB-CBD by 6.6-6.8 kcal mol^{-1} [14]. This failure is enhanced by B3LYP/6-31+G*//B3LYP/6-31G* slightly [3].

Considering the above situation, we reported the ground PESs between THD and CBD that was computed by CASSCF [4]. According to our results, THD to CBD isomerization occurs via a different route (Scheme 3) from the route previously suggested (Scheme 2). Both reaction processes involve exo-bicyclodiradical species. We considered that this reaction process (Scheme 3) is preferable than the previously suggested one (Scheme 2) because the reaction process of Scheme 2 is influenced by bulky substituents more strongly than Scheme 3 due to the involvement of the *endo* species.

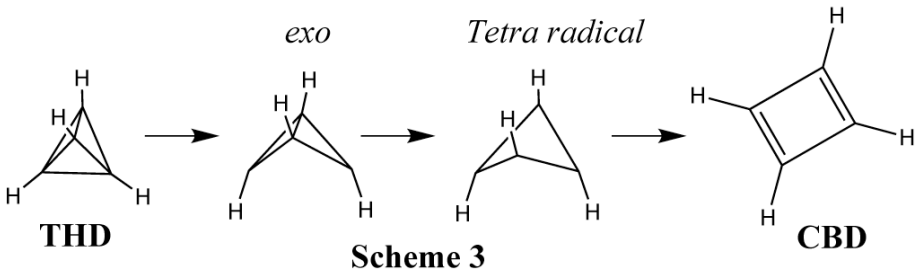

Scheme 3

This paper deals with this issue. According to the present calculation, σ-donating electronic effect by *tert*-butyl groups rather than steric repulsion between them plays an important role when TB-CBD isomerizes to TB-THD on the HOMO/LUMO double-electron excited state, while in the ground state, the steric repulsion between *tert*-butyl groups overcomes electronic effect of *tert*-butyl group.

2. Computational Details

Geometry optimization, minimum-energy-path (MEP), and intrinsic reaction coordinate (IRC) calculations were performed using the complete active space self-consistent filed (CASSCF) method implemented in GAUSSIAN03 [15]. The feature of CASSCF is the flexibility in selecting an appropriate active space. We need to select orbitals as an active space suitably. To describe the six equivalent σ bonds of THD accurately, twelve electrons in twelve orbitals are preferable as an active space. However, such active space is demanding even for modern computers. Therefore, the whole π system that corresponds to that of the parent CBD is employed as the active space. We expected that the result in this paper [CAS(4,4)] would not differ

significantly from that of CAS(12,12) because, in this paper, we don't deal with the breakage of the σ bonds that constructs the original σ bonds of CBD.

Considering computational resource, we used two types of basis sets depending on the purpose of calculation: a mixed basis (MixB) or 6-31G*. MixB adopts 6-31G* to the four-membered ring carbon atoms and STO-3G to the other carbons and hydrogen atoms and was used for structure optimization, and IRC and MEP calculations. To calculate more precisely energies at fixed structures, 6-31G* basis set was employed in multi-reference based calculations described below.

CASSCF takes into account the static electronic correlation, but not dynamic electronic correlation properly. The results of the CASSCF calculation show that electronic structures have multi-configuration properties at some stationary points on the S_0 PES we have located. This means that multi-reference calculation is suitable to reinforce the CASSCF energy. Hence, to improve the computed energetics by incorporating the effect of the dynamic electronic correlation, we carried out single point calculations using multi-reference Møller-Plesset second-order perturbation (MRMP2) [16] implemented in GAMESS [17] on the geometries optimized for energy

by CASSCF/MixB. A reference CASSCF/6-31G* wave function with the same active space described above was used for all MRMP2 calculations. The weights of states in MRMP2 were equally assigned for three states (S_0, S_1 and S_2). When we explored the reactive excited states of TB-CBD, the vertically excited energies of the lowest five states (S_0, S_1, S_2, S_3, and S_4) were calculated with equal weights of states.

Energetic degeneracy between electronic states can be regarded as not only a point but also space. We take the degeneracy between two states having the same spin multiplicity as the instance. At a degeneracy point, two degeneracy lifting vectors can be defined. One is the gradient difference vector (GD) and the other is the derivative coupling vector (DC). Conically intersected PESs can be described as the function of GD and DC. Namely, the real crossing between PESs having the same spin-multiplicity is called a conical intersection (CI). Here, the degeneracy point is given as the apex of the CI. In the recent computational photochemistry, it is not doubtful CIs play a crucial role [18-21]. However, there is no isolated degeneracy point except for diatomic molecules. In the complement space to the GD and DC [(n−2)-dimensional space (here n is the number of the internal degree of freedom of a molecule)], the degeneracy is kept

[20,21]. This (n−2)-dimensional degeneracy space (DS) is often called a CI hyperline or seam [20,21]. In this paper, we call it a DS simply.

The nature and influence of DSs to the photochemistry are still poorly understood. Sometimes, photochemically different CIs exist in the same DS [23-25]. In such cases, it is not sufficient to carry out the MEP calculation at the CASSCF level, but is necessary to search a photochemically different CI in the same DS and explore the route to the CI. Hence, we carried out the DS scan as a function of an internal coordinate of the molecule. Though there are some methods to scan DS along an internal coordinate [22], we employed the two-step method [23].

3. Results and Discussion

To calculate the S_0 PES from the S_1/S_0 conical intersection is a great help to analysis of the reaction in the ground state [4]. Hence, at first, we discuss the photoreaction from TB-CBD to TB-THD, and next, thermo-reaction TB-THD to TB-CBD (reverse reaction) will be discussed.

3.1. Photoreaction from TB-CBD to TB-THD

3.1.1Vertical excitation energy of TB-CBD

The optimized geometry of TB-CBD by CAS/MixB is shown in Fig. 1. The parameters optimized by CAS/6-31G* is also shown in parentheses for comparison. Although we did not impose any symmetry in all calculations, TB-CBD has basically D_2 symmetry (out-of-plane distorted rectangle). There is no large difference between the geometries optimized by CAS/MixB and CAS/6-31G*. The double bonds of the four-membered ring at the CAS/MixB and CAS/6-31G* level are calculated as 1.372 and 1.373 Å, respectively, while the single bonds are 1.577 and 1.574 Å. Therefore, we justify that MixB is adequate. In comparison with the experimental result (1.441 and 1.527 Å for the double and single bonds) [2,26], the lengthes of the double bonds of the four-membered ring are underestimated. We know that this discrepancy between the experimental and CASSCF-calculated lengths will be diminished by adding the σ-orbitals of the four-membered ring to the active space [10]. Unfortunately, however, the present system is too large to expand the active space to the σ-orbitals. On the other hand, the present geometry optimized by CASSCF is closer to the experimental one

than that by DFT/B3LYP [3, 14]. Furthermore, the stability of the TB-CBD, i.e., TB-CBD is more stable than TB-THD [3, 13], is successfully reproduced at the CASSCF level as will be shown.

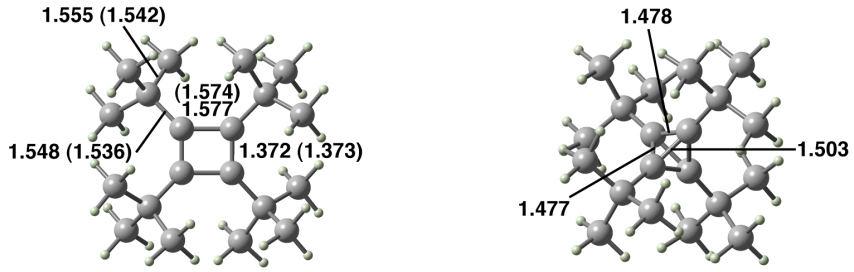

Figure 1. Optimized structure of TB-CBD (left) and TB-THD (right) by CAS/MixB. The values are given in Å. The values by CAS/6-31G* are also given in parentheses for TB-CBD. The experimental lengths of TB-CBD are 1.441 and 1.527 Å for the double and single bonds in the central four-membered ring. Because the six σ-bonds of the central tetrahedrane are not equal, this TB-THD has S_4 symmetry at most.

The electron configuration of TB-CBD by CASSCF gives the reason why the discrepancy between the DFT calculations [3, 14] and the experimental results [2,26] appears. See Fig. 2 for the representation of the electron configurations. According to our CASSCF calculation, $(b1)^2(b3)^2$ is the most dominant configuration (approximately 85%) and the second most dominant configuration is $(b1)^2(b2)^2$ (approximately 6%). The contribution of $(b1)^2(b3)^2$ configuration emphasizes the character of the double

bond and single bonds of the four-membered ring. On the other hand, $(b1)^2(b2)^2$ configuration completely offsets the effect of $(b1)^2(b3)^2$. We can predict that the methods based on a single configuration overestimates the character of single and double bonds of the four-membered ring due to the lack of the contribution of $(b1)^2(b2)^2$. Though the electron configuration of TB-CBD has the single configuration property, we concluded that a multi-configuration approach is necessary in this system.

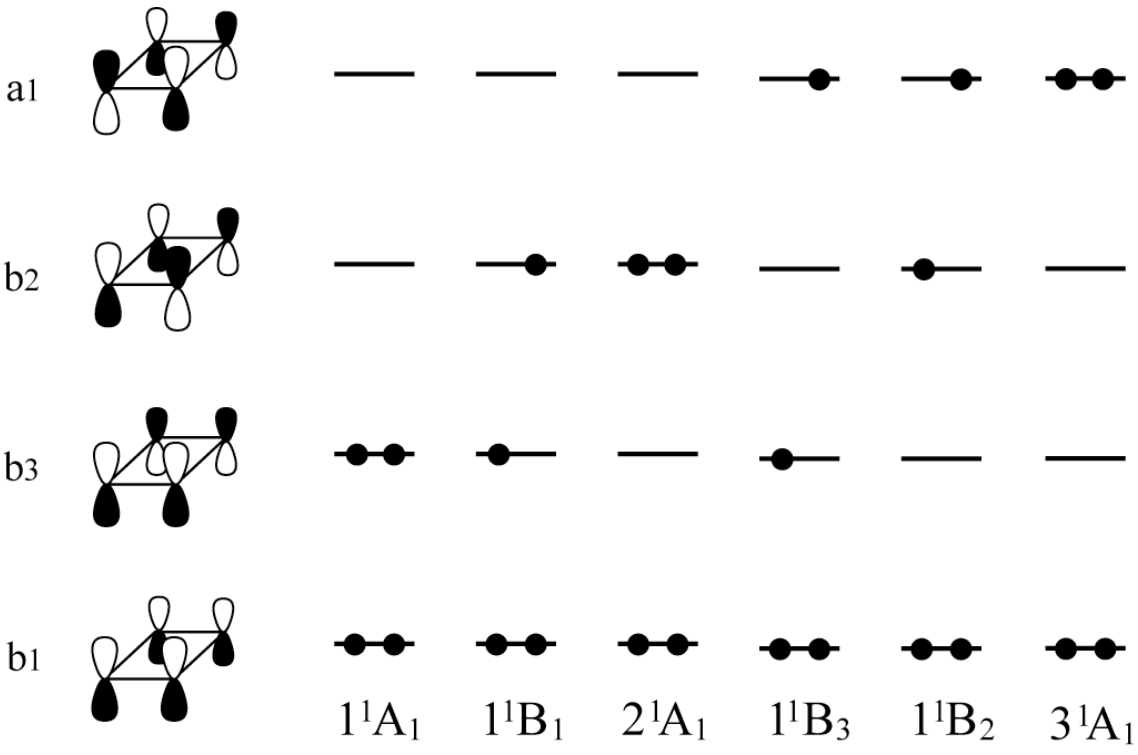

Figure 2. Classification of electron configurations in the π system of CBD derivatives assuming D_2 symmetry. Filled circle indicates an electron.

The vertical excitation energies of the lowest four valence excited state of TB-CBD were calculated as tabulated in Table 1. There, it is assumed for simplicity that TB-CBD has D_2 symmetry. Similarly to the case for the parent CBD, CASSCF cannot calculate the order of the excited states correctly [27,28] though the optimized geometry at the CASSCF level is comparable to the experimental results [2,26]. Hence, the energies obtained by MRMP2 are suitable for quantitative discussion.

Table 1. Vertical excitation energy (in eV) calculated by MRMP2/6-31G* and MRMP2/6-311G* on the structure optimized by CAS/6-31G* or CAS/MixB.

	CAS/MixB[a]		CAS/6-31G*[a]	
	6-31G*[b]	6-311G*[b]	6-31G*[b]	6-311G*[b]
1^1A_1	0.	0.	0.	0.
1^1B_1	2.70	2.51	2.62	2.44
2^1A_1	3.17	3.09	3.00	2.92
1^1B_3	4.88	4.29	4.99	4.39
1^1B_2	6.58	5.93	6.60	5.92

a) Method used in geometry optimization.

b) Basis set used in single point calculation with MRMP2.

Prior to comparison between computational and experimental results of energetics, we checked the dependence of the computational results on the basis set by comparing the results of double-zeta with that of triple-zeta. By using the larger basis set, the vertical excitation energies tend to lower for both the optimized geometries by CAS/MixB and CAS/6-31G*. Especially, the excitation energies to 1^1B_3 and 1^1B_2 states are notably lowered by changing the double-zeta to the triple-zeta basis set on both the optimized structures by CAS/MixB and 6-31G*. However, the vertically excited energy to the 1^1B_3 state (4.39 eV) with the optimized structure by CAS/6-31G* is larger than that by CAS/MixB (4.29 eV). This means that if we used the reliable geometry, the 1_1B_3 state is energetically elevated. Therefore, the actual vertical excited energy to the 1^1B_3 state is predicted to become larger than we have calculated.

According to the experimental result, TB-CBD is isomerized to TB-THD by irradiating light with > 300 nm (< 4.13 eV) [2,7]. There are two excited states under 4.13 eV as shown in Table 1. One is the symmetry allowed single-electron excited state, 1^1B_1 state, and the other the symmetry forbidden double-electron excited state, 2^1A_1 state. Therefore, the 1^1B_1 state seems to be the initial excited state for the TB-CBD to

TB-THD criss-cross reaction [2,7].

According to the computational result of the analogous reaction of cyclooctatetraene [28], the double-electron excited state becomes responsible for the photoreaction though the direct excitation to the double-electron excited state is improbable because the excited state is symmetry forbidden. Similarly, in the case of TB-CBD, the lowest excited state (1^1B_1) seems to be the initial excited state whereas the double-electron excited state seems to be the responsible state for the criss-cross reaction [2,7].

Our calculation indicates that no reaction occurs while TB-CBD stays in the HOMO/LUMO single-electron excited state because there is a minimum (S_2 min), which has almost D_{2d} symmetry, in that state as shown in Fig. 3. S_2 Min, located by geometry optimization starting from the Frank-Condon (FC) point of the HOMO/LUMO single-electron excited state, lies 29.5 kcal mol^{-1} below the FC point of the HOMO/LUMO single-electron excited state at the MRMP2//CASSCF level. The geometry optimization indicates the existence of the barrier-free route to S_2 Min in a similar way to the parent CBD [27, 28]. Furthermore, any transition states could not be

located around S_2 Min. This means that molecules are trapped around S_2 Min if they remain in 1^1B_1 state. Another states would be responsible for the photoreaction from TB-CBD to TB-THD, accordingly. It is plausible that the photoreaction of TB-CBD occurs via the double-electron excited state (2^1A_1 state) after the direct excitation to the symmetry allowed single-electron excited state, i.e., 1^1B_1 state as we suggested based on our qualitative discussion [10]. Indeed, this prediction will be proved throughout this paper.

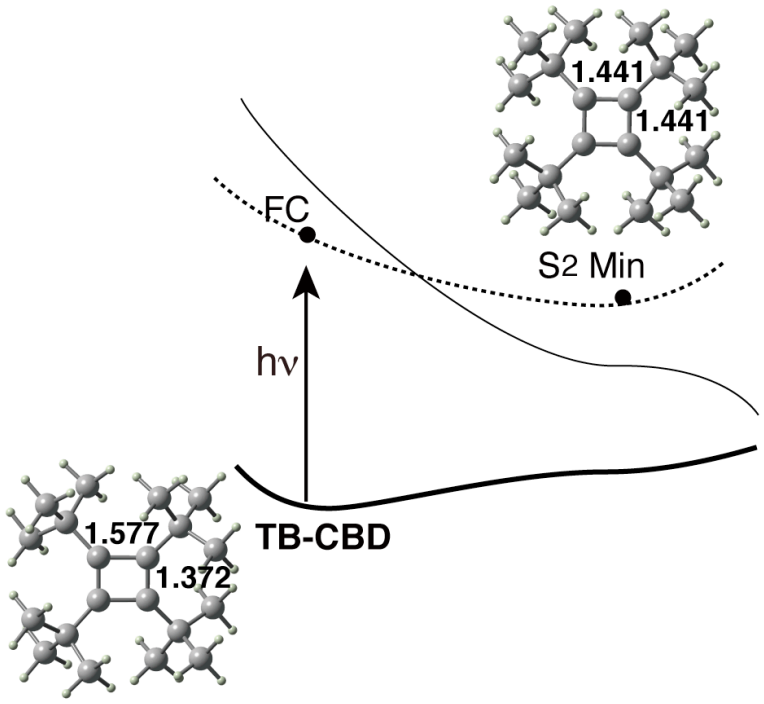

Figure 3. Schematic potential energy surface around the minimum in the S_2 state (S_2 Min). Bold, dashed, and plain lines indicate the PESs of the ground, HOMO/LUMO single-electron excited, and HOMO/LUMO double-electron excited state, respectively. Bond lengths are given in Å. There are minimum (S_2 Min), which lies 29.5 kcal mol^{-1} below the Frank-Condon point (FC) at the MRMP2//CASSCF level, on the HOMO/LUMO single-electron excited state PES. The four bonds of four-membered ring at S_2 Min are equal to 1.44 Å.

3.1.2 Minimum-energy-path calculation in the excited state

MEP calculations from a FC point (vertically excited point) is a useful tool to search the major reaction path [18, 19]. The reaction path obtained by MEP calculation can be used for prediction for the results of the trajectory calculation [30]. We carried out the MEP calculation for 2^1A_1 state by MRMP2/6-31G*//CAS/MixB. As already mentioned, the 2^1A_1 state is artificially calculated as the S_1 state around the equilibrium structure of TB-CBD at the CASSCF level. Hence, this S_1 MEP is calculated as the possible path where the transition from the 1^1B_1 (HOMO/LUMO single-electron excited state) to 2^1A_1 state (HOMO/LUMO double-electron excited state) occurs. More accurately, the PESs calculated by MRMP2//CASSCF indicated that the single-electron excited state intersects the double-electron excited state at the early step of the MEP as shown in Fig. 4 without barrier at approximately 0.4 Bohr $amu^{1/2}$ by slight geometrical deformation from rectangular to rhomboid and square TB-CBD. Consequently, the region where the HOMO/LUMO single-electron excited state is the S_1 state is limited to around the FC points. This tendency is in good agreement with the case of the parent CBD [10,27,28].

After the S_2/S_1 crossing, the excited TB-CBD reaches the energetically flat region

(approximately 0.99-3.52 Bohr amu$^{1/2}$) by the deformation from out-of-plane rectangle to rhomboid. Around this region, the slight deformation by the pyramidalization of carbon atoms also occurs. In the case of the parent CBD, the excited CBD reaches the S_1/S_0 CI by the pyramidalization of carbon atoms. However, the double-electron excited TB-CBD does not reach a S_1/S_0 CI by the same deformation. The stabilization energy up to 3.52 Bohr amu$^{1/2}$ is 43.1 kcal mol^{-1}, which is smaller than that of the S_1 parent CBD up to S_1/S_0 CI (65.7 kcal mol^{-1}) [10]. Furthermore, the degree of the geometric relaxation is not enough in comparison with the case of the parent CBD. That is, the sums of the bond angle around carbon atoms are 356.6°and 338.3° at the terminal point (TP) of S_1 MEP of the parent CBD. However, those for the four-membered ring of TB-CBD at the S_1 saddle point (SP) are 357.9° (C1, C3) and 358.1° (C2, C4) as shown in Table 2. Hence, it is clear that the steric repulsion prevents the S_1 TB-CBD from stabilizing energetically. This steric repulsion between *tert*-butyl groups holds up TB-CBD in S_1 state.

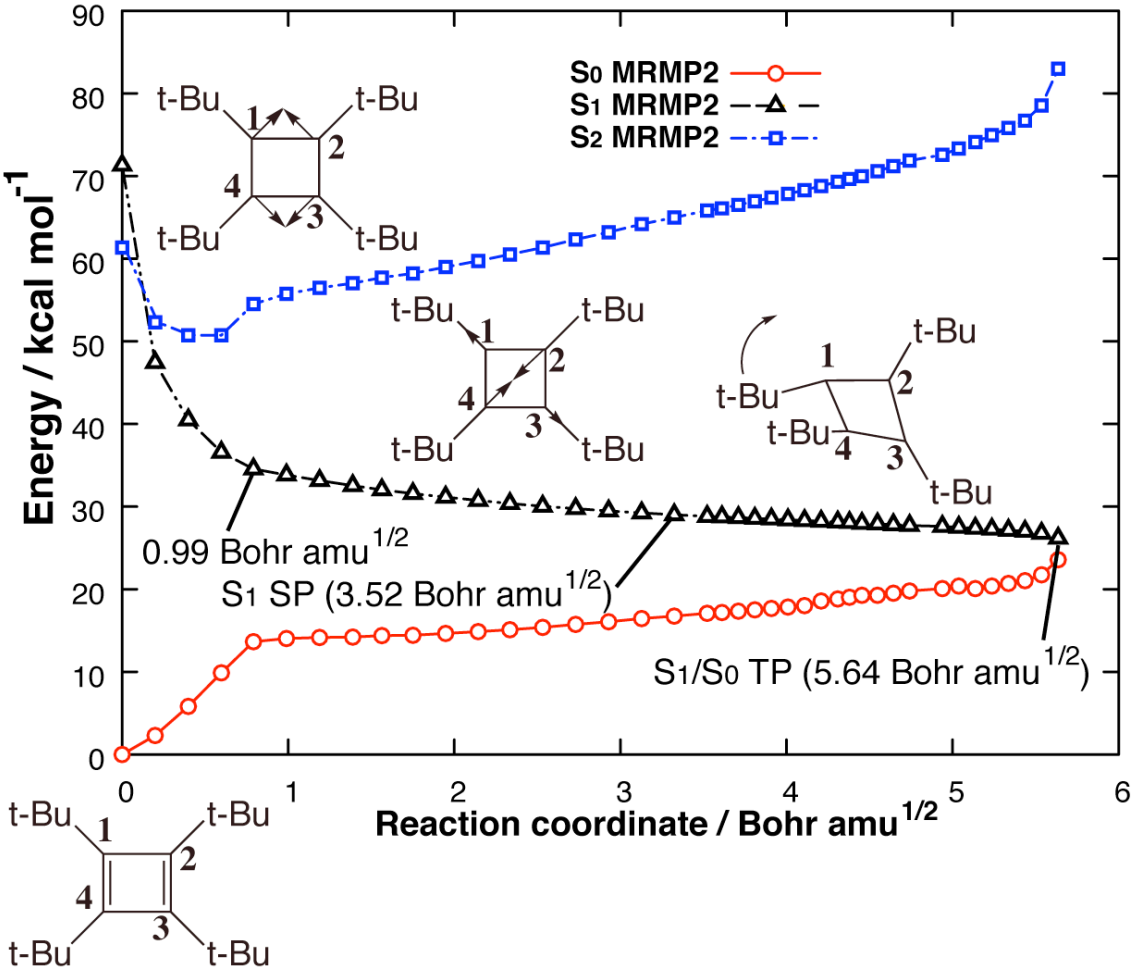

Figure 4. MRMP2/6-31G*//CASSCF/MixB energy profile of minimum energy path (MEP) from the Franck–Condon (FC) point of the double-electron excited state of TB-CBD. The order of states is described by that obtained by CASSCF. Quadratization and rhomboidal distortion proceed up to approximately 0.99 Bohr amu$^{1/2}$, then pyramidalization occurs [1.0 Bohr amu$^{1/2}$ to 3.52 Bohr amu$^{1/2}$ (S_1 SP)]. Finally, the rocking motion of one *tert*-butyl group (attached to C1) mediates the excited TB-CBD to reach S_1/S_0 conical intersection (S_1 TP).

Table 2. Geometric parameters of the four-membered ring of TB-CBD, S_1/S_0 conical intersections, and other stationary points optimized by CAS(4,4)/MixB in Gaussian03

	S_0 TB-CBD	S_2 Min	S_1 SP	S_1 TP	S_1/S_0 CI_{ionic}	S_1/S_0 CI_{tetra}	S_0 TS_1	S_0 TS_2	S_0 TB-THD
					Bond length (Å)				
C1-C2	1.577	1.441	1.459	1.465	1.470	1.465	1.482	1.403	1.478
C2-C3	1.372	1.441	1.459	1.453	1.445	1.506	1.455	1.496	1.477
C3-C4	1.577	1.441	1.459	1.453	1.445	1.501	1.482	1.527	1.478
C4-C1	1.372	1.441	1.459	1.465	1.470	1.506	1.455	1.462	1.477
C1-C3	2.089	2.035	2.168	2.180	2.205	2.050	1.776	1.981	1.503
C2-C4	2.089	2.035	1.934	1.906	1.838	2.055	2.247	1.981	1.503
					Sum of the bond angles around carbon atoms of four-membered ring (°)				
Σ_{C1}	357.7	357.4	357.9	357.4	350.6	351.5	354.1	359.8	350.3
Σ_{C2}	357.7	357.4	358.1	358.5	358.2	351.4	346.0	359.8	350.3
Σ_{C3}	357.7	357.4	357.9	351.2	345.5	343.7	354.1	335.1	350.3
Σ_{C4}	357.7	357.4	358.1	358.5	358.2	343.6	346.0	335.1	350.3
					Dihedral angle (°)				
C1-C2-C3-C4	-6.4	-6.8	-9.0	-14.1	-20.0	-27.1	-25.3	-36.3	-69.6

Table 3. Mulliken charges of carbon atoms of the four-membered ring calculated by CASSCF/MixB at each species in atomic units

	S_0 TB-CBD	S_2 Min	S_1 TB-CBD	S_1 SP	S_1 TP	S_0 TS_1	S_0 TS_2	S_0 TB-THD
C1	–0.0277	–0.0343	–0.1721	–0.2528	–0.2149	–0.0339	–0.0080	–0.0175
C2	–0.0277	–0.0343	0.0967	0.1927	0.1666	–0.0474	–0.0080	–0.0175
C3	–0.0277	–0.0343	–0.1721	–0.2528	–0.2553	–0.0339	–0.0529	–0.0175
C4	–0.0277	–0.0343	0.0967	0.1927	0.1667	–0.0474	–0.0529	–0.0175

From 3.52 Bohr amu$^{1/2}$ (S_1 SP), the TB-CBD is stabilized by the rocking motion of one *tert*-butyl group (attached to C1). Finally, the S_1 TB-CBD reaches the S_1/S_0 CI at the TP of the S_1 MEP (the S_1/S_0 energy difference is only 2.60 kcal mol^{-1}). The ionic electronic structure is exhibited because C1 and C3 atoms have large negative charges (−0.253 a.u. shown in Table 3). The stabilization energy by this rocking motion is only 2.65 kcal mol^{-1}. Total stabilization energy from the FC point to the S_1 TP is 45.8 kcal mol^{-1}, which is still smaller than the stabilization energy of the parent CBD from FC point to the TP of S_1 MEP (65.7 kcal mol^{-1}) [10]. Therefore, the relaxation of the four-membered ring of TB-CBD is incomplete due to the steric repulsion between *tert*-butyl groups.

To get the optimized structure in the $n-2$ dimensional DS, we carried out the geometry optimization from the TP of the S_1 MEP. Some geometric parameters at the S_1/S_0 CI are tabulated in Table 2. This structure is analogous to the minimum on the S_1 PES of the parent CBD optimized by MR-AQCC [31]. However, according to our calculation on TB-CBD, it is not the minimum but an S_1/S_0 CI. Clearly, this structure reflects the ionic electronic structure at the FC point because the degree of

pyramidalization of C1 and C3 (Σ_{C1}=350.6, Σ_{C3}=345.5) is enhanced in comparison with the S_1 TP as shown in Table 2 (Σ_{C1}=357.4, Σ_{C3}=351.2). Therefore, we refer this CI as S_1/S_0 CI_{ionic}. The energy difference between S_0 and S_1 is 14 kcal mol^{-1} at the MRMP2/6-31G*//CAS/MixB level (see the supplementary data). This energy difference makes us to doubt the existence of S_1/S_0 CI. However, the existence of the CI_{ionic} is certain because the S_1/S_0 energy difference at the TP of the S_1 MEP is 2.6 kcal mol^{-1}. The detailed geometry of CI_{ionic} severely depends on the dynamic electronic correlation.

The GD and DC vector at S_1/S_0 CI_{ionic} are shown in Fig. 5 with those at S_1/S_0 CI_{ionic} of the parent CBD. The DC at CI_{ionic} indicates the bond alternation mode and the GD indicates the pyramidalization/planarization of carbon atoms. There is no large difference between the parent CBD and TB-CBD in these vectors. In the case of the parent CBD, no reaction occurs except for the automerization [4]. Therefore, it is unlikely that other reactions except for the automerization occur if CI_{ionic} is related to the photoreaction of TB-CBD. Indeed, geometry optimizations from S_1/S_0 CI_{ionic} indicate that the only bond alternation occurs similarly to the case of the parent CBD.

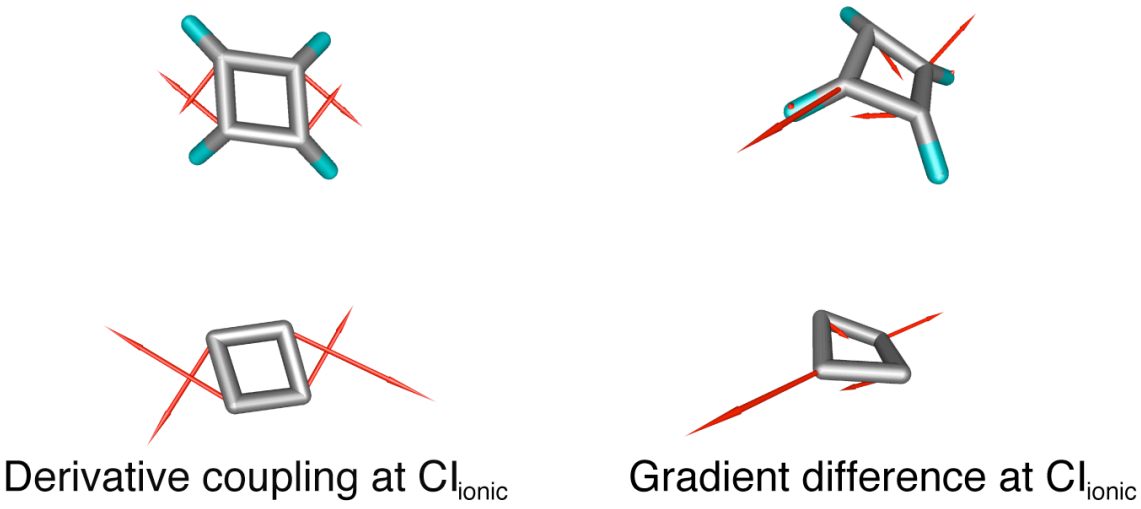

Figure. 5. Derivative coupling (left) and gradient difference (right) vectors at CI_{ionic} of TB-CBD (upper) and CBD (lower) [10]. For clarity, the *tert*-butyl groups of TB-CBD are removed. Derivative coupling vectors indicate the bond alternation of the four-membered rings. Gradient difference vectors indicate the pyramidalization/planarization. There is no large difference between the vectors of TB-CBD and CBD.

3.1.3 Exploring S_1/S_0 degeneracy space

Contrary to our expectation, the TP of the S_1 MEP does not become the channel for the reaction from CBD to THD even if hydrogen atoms of the parent CBD are replaced by *tert*-butyl groups. Hence, the main reaction path of TB-CBD via the double-electron excited state is the bond alternation at the present calculation level. According to our qualitative predication, the channel from S_1 to S_0 for the criss-cross reaction [2,7] is tetra-radical CI (CI_{tetra}) [10]. We found S_1/S_0 CI_{tetra} by exploring the S_1/S_0 degeneracy space for the parent CBD. Here we assess a similar possibility.

Staring from CI_{ionic} of TB-CBD, the S_1/S_0 DS of TB-CBD is explored along the simultaneous bond elongation of C1–C2 and C3–C4 up to 2.0 Å at the CASSCF level. The result is shown in Fig. 6 with the S_1/S_0 DSs of the parent CBD. We define the S_1/S_0 DS including CI_{ionic} as DS_{ionic} and that including CI_{tetra} as DS_{tetra}. Around C1–C2 (C3–C4) = 1.7 Å-1.8 Å, the change of the chemical character of the DS is expected because chemical characters of CIs in the same consecutive DS change at the energetic anomaly [23-25]. Indeed, beyond C1–C2 (C3–C4) = 1.8 Å, the result of calculation clearly converged to a different S_1/S_0 DS from the DS_{ionic} obtained up to C1–C2

(C3–C4) = 1.7 Å. Furthermore, we characterized the S_1/S_0 DS starting from this S_1/S_0 degeneracy point at 2.0 Å by contracting the bonds. This S_1/S_0 DS is energetically lower than DS_{ionic} around C1–C2 (C3–C4) = 1.6 Å. To get the energetic minimum in this S_1/S_0 DS, optimization in the DS was performed without any geometric constrain. We think that this structure is tetra-radical CI (CI_{tetra}) because sums of the bond angles carbon atoms of the four-memberd ring (Σ_{Ci}) showing less than 352° indicate that the carbon atoms are pyramidarized due to localized electron at each carbon atom (geometric parameters of the obtained structure are tabulated in Table. 2). Interestingly, C3 and C4 ($\Sigma_{Ci=1,2}$ = 344°) is more pyramidarized than C1 and C2 ($\Sigma_{Ci=1,2}$ = 351°) in contrast to the CI_{tetra} of the parent CBD, where four carbon atoms are equally pyramidarized. Furthermore, the C1−C2 bond seems to be getting the double bond character because it (1.47 Å) is shorter than the C3−C4 bond (1.51 Å). We consider that this nonequivalence of the four carbon atoms is due to mixing of the property of DS_{tetra} with that of DS_{ionic}. This tendency is also reflected in the GD and DC at CI_{tetra} of TB-CBD.

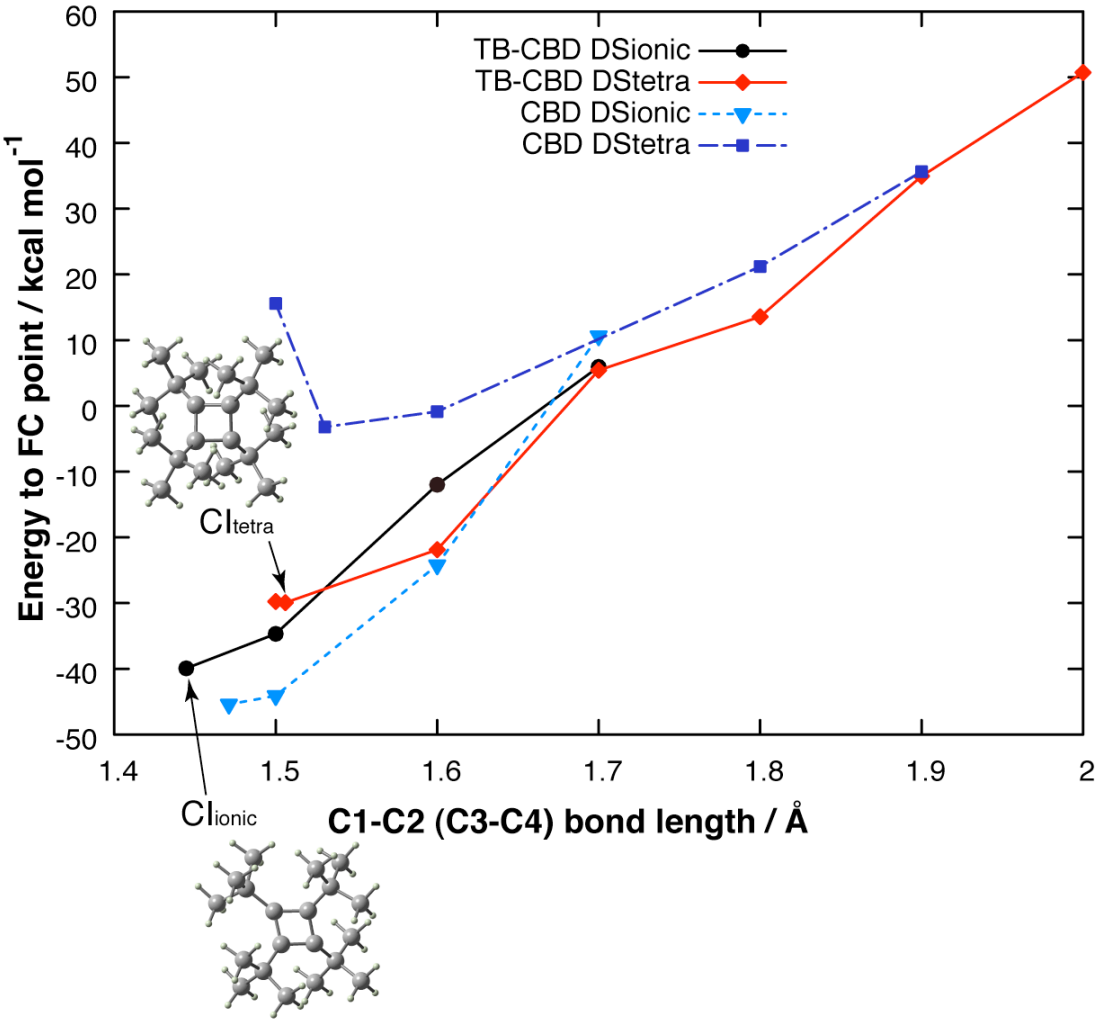

Figure 6. Relative energies of S_1/S_0 degeneracy spaces with respect to the vertically excited points of the HOMO/LUMO double-electron excited state explored by CASSCF level along simultaneous elongation/contraction of C1–C2 and C3–C4 bonds with those of the parent CBD by CAS/cc-pVDZ [10]. DS_{ionic} continues up to C1–C2 (C3–C4) = 1.7 Å, beyond which DS_{tetra} is obtained.

The GD and DC at CI_{tetra} of TB-CBD are shown in Fig. 7 with those at CI_{tetra} of the parent CBD. The DC of TB-CBD shows the diagonal carbon atoms of the four-membered ring partly intersect similarly to the DC of CBD. Therefore, the CI_{tetra} of TB-CBD is the channel to TB-THD as already suggested on the basis of our previous calculation for the parent CBD [4,10]. On the other hand, the GD of TB-CBD at CI_{tetra} is largely different from that of the parent CBD. The GD of TB-CBD is a mixed mode of the pyramidalization of two neighboring carbon atoms and the bond alternation. This mode leads to the ionic transition state (TS) we previously suggested; electrons are biased to neighboring two carbon atoms [4]. As will be shown, we find two TSs that are related to the reaction between TB-CBD and TB-THD in the direction of the DC and GD at CI_{tetra}.

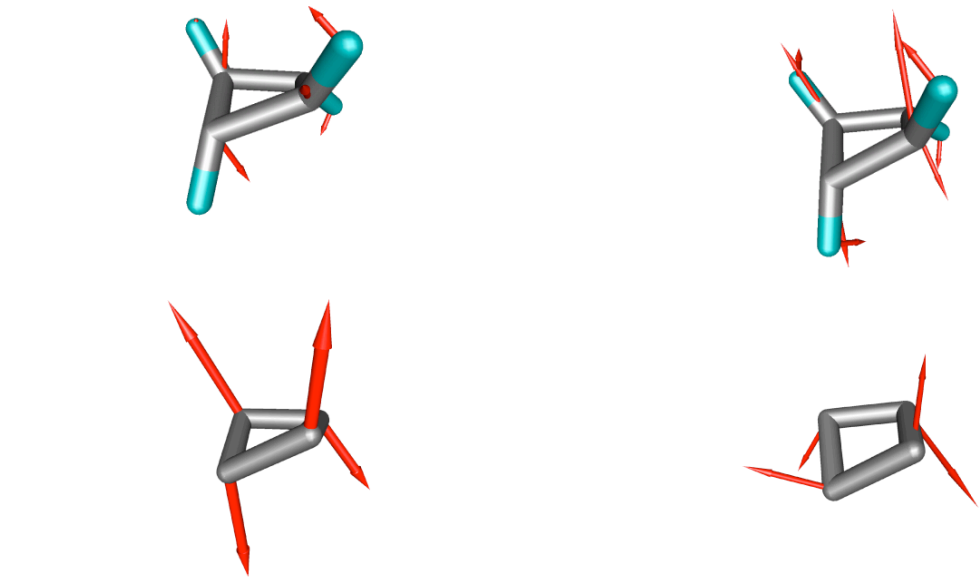

Figure 7. Derivative coupling (left) and gradient difference vector (right) at CI_{tetra} of TB-CBD (upper) and CBD (lower) [10]. For clarity, the *tert*-butyl groups of TB-CBD are removed. Derivative coupling vectors at CI_{tetra} of both TB-CBD and CBD indicates the pyramidalization mode of the four-membered ring. Gradient difference vector of TB-CBD indicates the mixing of bond alternation and pyramidalization modes whereas that of CBD indicates the pure pyramidalization mode.

Comparing the S_1/S_0 DSs of TB-CBD with those of the parent CBD, the DS_{tetra} of TB-CBD is extremely stabilized whereas the DS_{ionic} of TB-CBD is destabilized. It is well known that *tert*-butyl group stabilizes a radical electron by hyper-conjugation. Probably, *tert*-butyl groups stabilize the S_1 state of TB-CBD that has tetra-radical character. Similarly, the S_1/S_0 DS_{tetra} of TB-CBD is stabilized as shown in Fig. 8. In contrast, the ionic S_1 state of CBD is destabilized by *tert*-butyl groups because lone-pair electrons are destabilized. Consequently, CI_{tetra} (as the minimum point in DS_{tetra}) of TB-CBD is energetically close to CI_{ionic} (as the minimum point in DS_{ionic}) of TB-CBD. CI_{ionic} lies 41.0 kcal mol^{-1} below the FC point of the HOMO/LUMO single-electron excited state whereas CI_{tetra} lies 20.3 kcal mol^{-1} at the MRMP2//CASSCF level. This CI_{tetra} is energetically low enough for the HOMO/LUMO single-electron excited TB-CBD to access from the FC point.

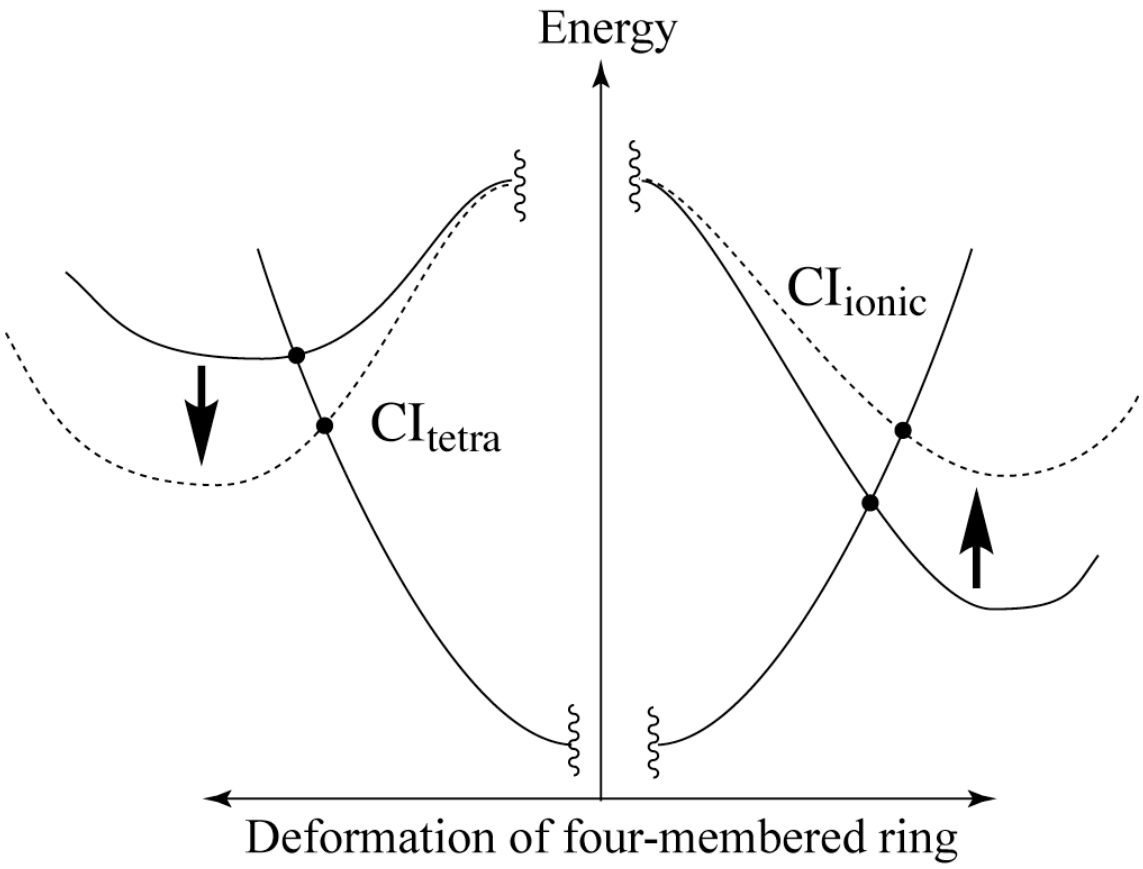

Figure 8. Schematic S_1/S_0 potential energy surfaces. The left one indicates the PES, which has tetra-radical like property. The right one indicates the PES, which has ionic like property. PESs of the parent CBD are drawn by solid lines while those of TB-CBD by broken lines. Replacing hydrogen atoms with *tert*-butyl groups destabilizes ionic state and stabilizes tetra-radical state. Arrows indicate that the stabilization or destabilization by replacing hydrogen atoms with *tert*-butyl groups. Consequently, DS_{tetra} illustrated in Fig. 6 energetically get closer to DS_{ionic}. At least, one barrier should exit between CI_{tetra} and CI_{ionic} because both CI_{tetra} and CI_{ionic} are peaked CI.

3.1.4 Path to S_1/S_0 CI_{tetra}

As shown in the previous section, CI_{tetra} of TB-CBD is energetically low enough to be accessible from the FC point of the HOMO/LUMO single-electron excited state. The remaining issue is whether the path to S_1/S_0 CI_{tetra} exists or not. According to our calculation, both CI_{ionic} and CI_{tetra} are peaked CI [32]. Therefore, at least, one barrier should exist between CI_{ionic} and CI_{tetra} as shown in Fig. 8. This barrier is expected to be a transition state, which connects ionic and tetra-radical electronic structure.

The MEP calculation in Fig. 4 shows the energetically flat region around 1.0-5.6 Bohr $amu^{1/2}$. While the double-electron excited TB-BCD hangs around here, electronic structure possibly change from ionic to tetra-radical. Starting from the SP on the S_1 PES (S_1 SP), a path up to the S_1/S_0 CI_{tetra} of TB-CBD was explored. As already mentioned, more than one barrier should exist between CI_{ionic} and CI_{tetra} because they are peaked CIs as shown in Fig. 8. Unfortunately, we failed to locate the barrier as the transition state by the optimization strategy. Instead, the relaxed scan between the S_1 SP and CI_{tetra} was performed while the geometry of the four-membered ring fixed to the structure obtained by linear interpolation between the S_1 SP and CI_{tetra}. The result is shown in Fig.

9. One barrier appeared. Because this barrier lies more than 20 kcal mol^{-1} below the FC point of the HOMO/LUMO single-electron excited state at the MRMP2/6-31G*//CAS/MixB level, the excited TB-CBD can overcome this barrier easily. Consequently, it is possible for TB-CBD to reach the S_1/S_0 CI_{tetra} via the HOMO to LUMO double-electron excited state. Now, we have proved that our prediction [10] is right, that is, the HOMO to LUMO double-electron excited state (1^1A_1 state) is a plausible reaction state for the photoreaction from TB-CBD to TB-THD.

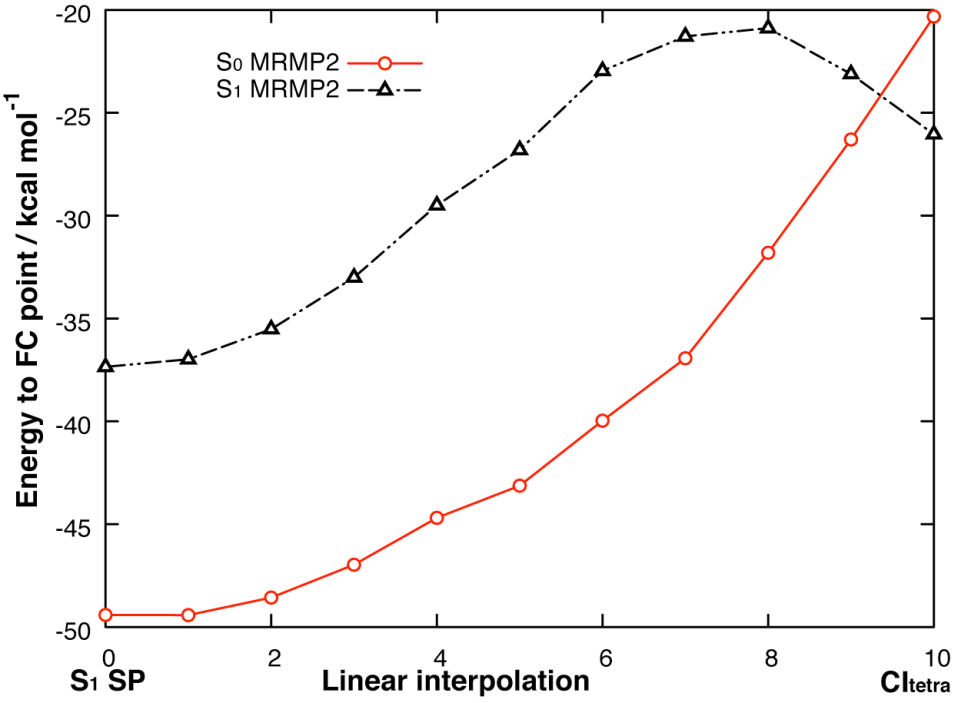

Figure 9. Energy profile by MRMP2/6-31G*//CAS/MixB between S_1 SP and S_1/S_0 CI_{tetra} of TB-CBD. The energy is relative to the Franck-Condon (FC) point of the HOMO/LUMO single-electron excited state. The coordinates of carbon atoms in the four-membered ring are obtained by the linear interpolation between S_1 SP and S_1/S_0 CI_{tetra}.

3.1.5 After decay from S_1/S_0 CI_{tetra}

The S_0 MEP calculation from S_1/S_0 CI_{tetra} of TB-CBD failed at 3.1 Bohr $aum^{1/2}$. Instead, geometry optimization was performed from S_1/S_0 CI_{tetra}. We have obtained TB-THD in consequence, suggesting that S_1/S_0 CI_{tetra} is the channel to TB-THD. The structure of TB-THD is shown in Fig. 1. According to the previous DFT calculation [14], TB-THD with T symmetry is more stable than that with T_d symmetry. The optimized structure in this study has approximately S_4 symmetry because six σ-bonds are not equal due to the lack of the active space. However, if six σ-bonds are equal, it is reasonable to regard the obtained structure has T symmetry.

In contrast to the DFT calculation [3,13], on the other hand, the present MRMP2//CASSCF calculation successfully reproduce the stability of TB-CBD. That is, TB-CBD is more stable than the TB-THD [3, 13]. According to our result, the relative energy of TB-THD with respect to TB-CBD is 2.2 kcal mol^{-1}, which is good agreement with the experimental results (ca. 2.39 kcal mol^{-1}) [3, 13].

We have also located the TSs for the TB-THD to TB-CBD isomerization from the

CI_{tetra}. One is located in the direction of the DC at the CI_{tetra}. This TS is defined as S_0 TS_1 at which two diagonally opposite carbon atoms (C2 and C4) have sp^3-hybridized character ($\Sigma_{Ci=2,4}$ = 346°) in contrast to the C1 and C3 showing sp^2-hybridized character ($\Sigma_{Ci=1,3}$ = 354°). However, the bias of charge in the four-membered ring is not observed (see Table 3). Hence, TS_1 has bicyclodiradical-like structure (pyramidarized diagonal carbon atoms and short C1−C3 length), which is analogous to that located by Kollmar et al [11]. TB-CBD is connected with TB-THD via S_0 TS_1.

The other TS is located in the direction of the GD at the CI_{tetra}. This TS is defined as S_0 TS_2. As shown in Table 2, the neighboring carbon atoms (C3, C4) are pyramidarized ($\Sigma_{Ci=3,4}$ = 335.1°) and the other neighboring carbon atoms (C1, C2) are almost planar ($\Sigma_{Ci=3,4}$ = 359.8°) at S_0 TS_2. Furthermore, Mulliken charges of C3 and C4 are −0.05285, which is more significant than C1 and C2 (−0.00798 a.u.). Therefore, TS_2 is the ionic TS as we have already predicted its existence [4].

3.2 Thermo-reaction from TB-THD to TB-CBD

As described in the previous section, two reaction routes from TB-THD to TB-CBD

were found on the S_0 PES. One is the route via TS_2 at which electrons are biased to the neighboring two carbon atoms of the four-membered ring. Energy diagrams are shown in Fig. 10. The other is the route via TS_1, which has bicyclodiradical structure.

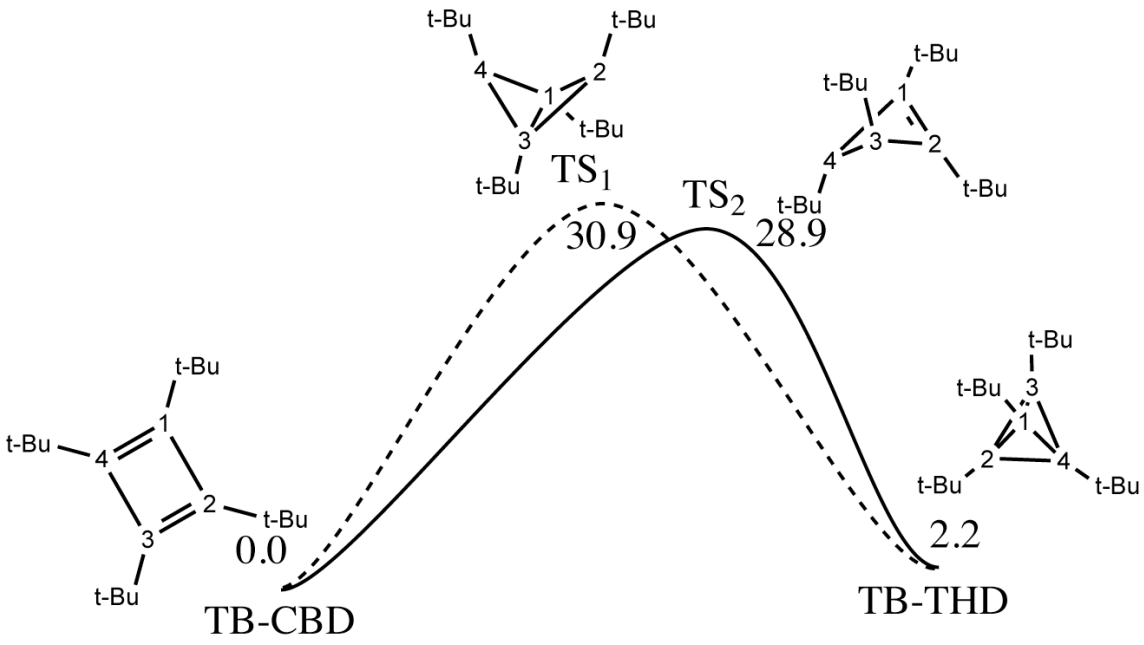

Figure 10. Energy diagram between TB-THD and TB-CBD. The value is relative energy (in kcal mol^{-1}) with respect to S_0 TB-CBD calculated by MRMP2/6-31G*//CAS/MixB. The atomic numbering for the carbon atoms of the four-membered ring, corresponding to that of Table 2, is also shown. TS_2 (biased ionic) is slightly lower than TS_1 (bicyclodiradical).

According to the IRC calculation at the CAS/MixB level, there is only one TS in each of reaction routes in contrast to the previous suggestions [4, 11]. TS_1 and TS_2 lie at 28-31 kcal mol^{-1} above TB-CBD and 26-28 kcal mol^{-1} above TB-THD. In comparison with the rate controlling TSs of the parent CBD/THD system [4], there is no large difference from the side of THD (approximately 30 kcal mol^{-1}). From the side of CBD, however, there is a large difference (note that more than 60 kcal mol^{-1} in the case of the parent CBD). That is, the steric repulsion between *tert*-butyl groups elevates the energy, i.e., the steric repulsion in TB-CBD is estimated as ca. 30 kcal mol^{-1} in energy. At the MRMP2/6-31G*//CAS/MixB level, TS_2 is energetically lower than that of TS_1 by 2.0 kcal mol^{-1} though TS_2 is less stable than TS_1 at the CAS/MixB level. Therefore, the reaction route via TS_2 would be dominant rather than that via TS_1.

In the case of the reaction route from the parent THD to CBD, the bicyclodiradical TS is slightly more stable than the biased ionic TS. Generally, *tert*-butyl group is known as σ-donating group that has the effect stabilizing the radical electron. Therefore, in the case of reaction route from TB-THD to TB-CBD, the bicyclodiradical species (TS_1) is more stabilized electronically than the biased ionic species (TS_2). However, the

bicyclodiradical species (TS_1) is energetically higher than biased ionic species (TS_2). This means that the destabilization by the steric repulsion between *tert*-butyl groups overwhelms the electronic stabilization by *tert*-butyl groups. Accordingly, the tetra-radical species, which have found by us [4], does not appear in the reaction route via TS_2. *Endo* bicyclodiradical species also does not appear in the reaction route via TS_1. If the electronic effect were stronger than the steric repulsion, these radical species would appear in the reaction route. However, these species does not appear due to the steric repulsion induced by *tert*-butyl groups. Therefore, tetrahedral shape (TB-THD) is certainly stabilized by steric-repulsion between *tert*-butyl groups rather than electronic effect on the S_0 PES.

4. Conclusion

We have investigated the photoreaction from TB-CBD to TB-THD (criss-cross reaction) [2,7] and thermo-reaction from TB-THD to TB-CBD by using MRMP2//CASSCF method. After the initial excitation to the HOMO/LUMO single-electron excited state, the reaction from TB-CBD to TB-THD occurs via the

HOMO/LUMO double-electron excited state (2^1A_1) in accordance with our qualitative predication [10]. Unfortunately, the dominant reaction via the double-electron excited state is automerization of TB-CBD. However, there is an important S_1 to S_0 channel to TB-THD, that is CI_{tetra}, which is energetically lower in comparison with that of the parent CBD by the electronic effect of *tert*-butyl groups. Furthermore, the HOMO/LUMO double-electron excited TB-CBD can easily reach CI_{tetra} over a small barrier. Therefore, we conclude that the TB-CBD to TB-THD photoreaction is possible via the HOMO to LUMO double-election excited state though its quantum yields might be small. The photoreaction from TB-CBD to TB-THD is schematically summarized in Fig. 11.

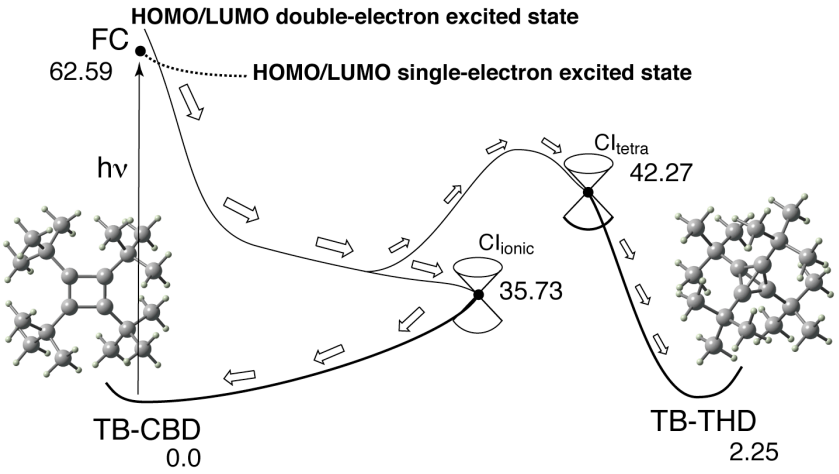

Figure 11. Schematic representation of the ground and HOMO/LUMO single/double-electron excited potential energy surfaces for the TB-CBD/TB-THD. The values are relative energies in kcal mol^{-1}. After vertically excited to the HOMO/LUMO single-electron excited state (FC), the HOMO/LUMO single-electron excited TB-CBD transits to the HOMO/LUMO double-electron excited state immediately. TB-CBD is then stabilized by the various deformations (bond alternation, pyramidalization, and rocking motion of one *tert*-butyl group). Finally TB-CBD reaches to CI_{ionic}, which is a channel for the automerizaiton of TB-CBD. On the way to CI_{ionic}, TB-CBD can reach CI_{tetra}, which is a channel to TB-THD, via a small barrier.

On the excited state, it is important for the possible reaction from TB-CBD to TH-THD that tetra-radical species is stabilized by the σ-donating effect of *tert*-butyl groups. On the other hand, in the ground state, the corset effect [2,5,6] induced by steric repulsion between *tert*-butyl groups seems to play an important role. The steric repulsion overcomes the electronic stabilization by the σ-donating effect of *tert*-butyl groups. Hence, many radical intermediate species, which were located in the parent CBD/THD system, disappear except for the bicyclodiradical TS (TS_1). Therefore, tetrahedral shape is surely stabilized by steric effect rather than electronic effect in contrast to the previous suggestion [5,6].

The previously suggested bicyclodiradical TS (TS_1) is located in spite of its diradical property. TS_1 lies 28.7 kcal mol^{-1} above TB-THD. This barrier is low enough to be overcome thermally. However, an energetically lower TS, that is TS_2, is also located at 26.6 kcal mol^{-1} above TB-THD. TS_2 is the ionic species that we previously predicted through qualitative consideration [4]. The thermoreaction from TB-THD to TB-CBD via TS_2 is probably dominant since TS_2 is energetically lower than TS_1 at our calculation level.

CBD/THD systems as photo-induced functional molecule are not enough if their function is induced via the process we suggested. However, we think there are sufficient potentials by improving the substituents. The present results demonstrate that the effect of substituents on CBD/THD differs considerably depending on electronic states. Naïve statements, though fascinating, would obscure the truth at least for CBD/THD because of delicate nature of their electronic states.

Appendix A. Supplementary material

The Cartesian coordinates at the S_0 equilibrium structure of TB-CBD, TB-THD, S_2 Min, CI_{ionic}, and CI_{tetra} are tabulated. Supplementary data associated with this article can be found, in the online version, at doi:###

References

[1] K. P. C. Vollhardt, N. E. Schore, Organic chemistry: structure and function, 3rd ed. 1998, W. H. Freeman and company.

[2] G. Maier, Angew. Chem. Int. Ed. Engl. 27 (1988) 309-332.

[3] R. Notario, O. Castaño, J. L. Andrés, J. Elguero, G. Maier, C. Hermann, Chem Eur. J. 7 (2001) 342-346.

[4] M. Sumita. K. Saito. Tetrahedron, 66 (2010) 5212-5217.

[5] (a) G. Maier, J. Neudert, O. Wolf, D. Pappusch, A. Sekiguchi, M. Tanaka, T. Matsuo, J. Am. Chem. Soc. 124 (2002) 13819-13826. (b) G. Maier, J. Neudert, O. Wolf, Angew, Chem. Int. Ed. 40 (2001) 1674-1675.

[6] M. Nakamoto, Y. Inagaki, M. Nishina, A. Sekiguchi, J. Am. Chem. Soc. 131 (2009) 3172-3173.

[7] G. Maier, S. Pfriem, U. Schäfer, R. Matusch, R. Angew. Chem. Int. Ed. Engle. 17 (1978) 520-512.

[8] (a) G. Maier, F. Fleishcer, H. –O. Kalinowski, Liebigs Ann. 1995, 173. (b) G. Maier, D. Bron, Angew. Chem. Int. Ed. Engl. 28 (1989) 1050-1052.

[9] S. Miki, T. Ena, R. Shimizu, H. Nakatsuji, Z. Yoshida, Tetrahedron Letters, 33 (1992) 1619-1620.

[10] M. Sumita, K. Saito, Chem. Phys. 371 (2010) 30-35.

[11] (a) H. Kollmar, F. Carrion, M. J. S. Dewar, R. C. Bingham, J. Am. Chem. Soc. 103 (1981) 5292-5303. (b) H. Kollmar, J. Am. Chem. Soc. 102 (1980) 2617-2621.

[12] B. O. Roos, in European Summer School in Quantum Chemistry; B. O. Roos, Ed. Lecture Notes in Quantum Chemistry; Springer: Berlin, Heidelberg, 1992; p177.

[13] G. Maier, S. Pfriem, K. –D. Malsch, H. -O Kailinowski, K. Dehnicke, Chem. Ber, 114 (1981) 3988.

[14] M. Balci, M. L. McKee, P. von R. Schleyer, J. Phys. Chem. A, 104 (2000) 1246-1255.

[15] M. J. Frisch, G. W. Trucks, H. B. Schlegel, G. E. Scuseria, M. A. Robb, J. R. Cheeseman, J. A. Montgomery, Jr., T. Vreven, K. N. Kudin, J. C. Burant, J. M. Millam, S. S. Iyengar, J. Tomasi, V. Barone, B. Mennucci, M. Cossi, G. Scalmani, N. Rega, G. A. Petersson, H. Nakatsuji, M. Hada, M. Ehara, K. Toyota, R. Fukuda, J. Hasegawa, M. Ishida, T. Nakajima, Y. Honda, O. Kitao, H. Nakai, M. Klene, X. Li, J. E. Knox, H. P. Hratchian, J. B. Cross, V. Bakken, C. Adamo, J. Jaramillo, R. Gomperts, R. E. Stratmann, O. Yazyev, A. J. Austin, R. Cammi, C. Pomelli, J. W. Ochterski, P. Y. Ayala, K. Morokuma, G. A. Voth, P. Salvador, J. J. Dannenberg,

V. G. Zakrzewski, S. Dapprich, A. D. Daniels, M. C. Strain, O. Farkas, D. K. Malick, A. D. Rabuck, K. Raghavachari, J. B. Foresman, J. V. Ortiz, Q. Cui, A. G. Baboul, S. Clifford, J. Cioslowski, B. B. Stefanov, G. Liu, A. Liashenko, P. Piskorz, I. Komaromi, R. L. Martin, D. J. Fox, T. Keith, M. A. Al-Laham, C. Y. Peng, A. Nanayakkara, M. Challacombe, P. M. W. Gill, B. Johnson, W. Chen, M. W. Wong, C. Gonzalez, and J. A. Pople, Gaussian, Inc., Wallingford CT, 2004. Gaussian 03, Revision D.02.

[16] H. Nakano, J. Chem. Phys. 99 (1993) 7983-7992.

[17] M. W. Schmidt, K. K. Baldridge, J. A. Boatz, S. T. Elbert, M. S. Gordon, J. H. Jensen, S. Koseki, N. Matsunaga, K. A. Nguyen, S. J. Su, T. L. Windus, M. Dupuis, J. A. Montgomery J. Comput. Chem. 14 (1993), 1347-1363.

[18] M. Olivucci, Computational Photochemistry, (Theoretical and Computational Chemistry vol. 16), (Ed: M. Olivucci) Elsevier

[19] A. Migani, M. Olivucci, In Conical Intersections: Electronic Structure, Dynamics & Spectroscopy (Advance Series in Physical Chemistry vol. 15), (Eds.: W. Domcke, D. R. Yarkony, H Köppel) World Scientific: Singapore, 2004, pp. 271.

[20] D. R. Yarkony, in Conical Intersections: Electronic Structure, Dynamics & Spectroscopy (Advance Series in Physical Chemistry vol. 15), (Eds.: W. Domcke,

D. R. Yarkony, H. Köppel) World Scientific: Singapore, 2004, pp. 41.

[21] F. Bernardi, M. Olivucci, M. A. Robb, Chem. Soc. Rev. 25 (1996) 321-328.

[22] F. Sicilia, L. Blancafort, M. J. Bearpark, M. A. Robb, J. Chem. Theory Comput. 4 (2008) 257-266.

[23] M. Sumita, K. Saito, J. Chem. Theory Comput. 4 (2008) 42-48.

[24] A. Venturini, T. Vreven, F. Bernardi, M. Olivucci, M. A. Robb, Organometallics 14 (1995) 4953-4956.

[25] I. J. Palmer, I. N. Ragazos, F. Bernardi, M. Olivucci, M. A. Robb, J. Am. Chem. Soc. 115 (1993) 673-682.

[26] H. Irngartinger, M. Nixdorf, Angew. Chem. Int. Ed. Engl. 22 (1983) 403-404.

[27] A. Balková, R. J. Bartlett, J. Chem. Phys. 101 (1994) 8972-8987.

[28] S. V. Levchenko, A. I. Krylov, J. Chem. Phys. 120 (2004) 175-185.

[29] M. Garavelli, F. Bernardi, A. Cembran, O. Castaño, L. M. Frutos, M. Merchán, M. Olivucci, J. Am. Chem. Soc. 124 (2002) 13770-13789.

[30] O. Weingart, A. Migani, M. Olivucci, M. A. Robb, V. Buss, P. Hunt, J. Phys. Chem. A, 104 (2004) 4685-4689.

[31] M. E-. Maksić, M. Vazdar, M. Barbatti, H. Lischka, Z. B. Maksić, J. Chem. Phys. 125 (2006) 064310-9.

[32] G. J. Atchity, S. S. Xantheas, K. Ruedenberge, J. Chem. Phys. 95 (1991) 1862-1876.

Supplementary data

For

Computational study on photo- and thermo-reactions between tetra-*tert*-butyl-substituted cyclobutadiene and tetrahedrane

Submitted by

Masato Sumita, Kazuya Saito, Yoshitaka Tateyama

Contents

Keywords

CASSCF, MRMP2, Cartesian coordinates, IRC

1. CASSCF and MRMP2 energies

Table S1. MRMP2/6-31G*//CASSCF/MixB and CASSCF/MixB energy for the S_2, S_1, S_0 stationary points and S_2/S_1, S_1/S_0 DP of TB-CBD.

Species	State	E_{CAS}[a]	E_{CAS}[b]	E_{MRMP2}[c]	E_{rel}[d]
S_0 TB-CBD	S_0	-770.94751		-780.84567	0.
	S_1			-780.74593	62.59
	S_2			-780.72708	74.42
S_2 Min	S_0			-780.83265	8.17
	S_1		-770.85194	-780.79299	33.06
	S_2		-770.79936	-780.77367	45.18
S_1 SP	S_0	-770.86234		-780.82756	11.36
	S_1			-780.79602	31.15
	S_2			-780.76111	53.06
S_1 TP	S_0	-770.86429		-780.822696	14.42
	S_1			-780.80400	26.14
	S_2			-780.74502	63.16
S_1/S_0 CI_{ionic}	S_0		-770.87085	-780.78873	35.73
	S_1		-770.87084	-780.81121	21.62
	S_2			-780.68006	103.92
S_1/S_0 CI_{tetra}	S_0		-770.85494	-780.78743	36.55
	S_1		-770.85491	-780.77831	42.27
	S_2			-780.71102	84.49
S_0 TS_1	S_0	-770.86565		-780.79635	30.95
	S_1	(281.8i)		-780.75386	57.61
	S_2			-780.71563	81.60
S_0 TS_2	S_0	-770.86348		-780.79967	28.87
	S_1	(612.5i)		-780.75509	56.84
	S_2			-780.71137	84.27
TB-THD	S_0	-770.93068		-780.84209	2.25

a) Single-state CASSCF energy in atomic units (computed by GAUSSIAN03). Values of imaginary frequency (cm^{-1}) are shown in parentheses.

b) Two-state-averaged CASSCF energy for S_0 and S_1 in atomic units (computed by GAUSSIAN03).

c) MRMP2 energy for S_0, S_1, and S_2 in atomic units (computed by GAMESS).

d) MRMP2 relative energy with respect to the S_0 equilibrium structure of CBD in kcal mol^{-1}.

2. Cartesian Coordinates located by CAS/MixB

S0 TB-CBD

C	0.053023	-0.036725	-0.052647
C	0.040307	-0.032255	1.319748
C	1.615960	0.018618	1.328527
C	1.613113	0.189304	-0.033276
C	2.599886	0.781856	-1.067950
C	2.672710	-0.393478	2.381546
C	-1.024165	0.249716	2.407305
C	-0.926028	-0.499145	-1.158549
C	3.620473	1.724479	-0.369985
H	4.235907	2.204330	-1.125835
H	3.099562	2.494600	0.187515
H	4.278059	1.197005	0.304039
C	3.366368	-0.312851	-1.857183
H	2.682808	-0.974274	-2.374644
H	4.015129	0.152691	-2.594476
H	3.978366	-0.910512	-1.192650
C	1.824794	1.694769	-2.059798
H	1.165350	1.133785	-2.704849
H	1.238559	2.428324	-1.517278
H	2.535173	2.222807	-2.689491
C	-1.687311	0.683438	-1.814835
H	-1.000347	1.402386	-2.243432
H	-2.330551	0.310922	-2.607737
H	-2.304334	1.196453	-1.087207
C	-1.951178	-1.518946	-0.587265
H	-2.560961	-1.903427	-1.400077
H	-1.433937	-2.351159	-0.123450
H	-2.613815	-1.076735	0.140964

C	-0.143428	-1.285506	-2.248096
H	0.520373	-0.650788	-2.815688
H	0.439231	-2.079628	-1.794243
H	-0.849033	-1.733073	-2.942200
C	-2.201824	1.074979	1.816245
H	-2.883916	1.345391	2.617465
H	-1.830249	1.985673	1.360386
H	-2.763648	0.524622	1.077044
C	-1.577997	-1.048997	3.051805
H	-0.783420	-1.637105	3.493707
H	-2.290582	-0.796204	3.832536
H	-2.082513	-1.661065	2.314119
C	-0.411001	1.159351	3.509365
H	0.343548	0.649897	4.089685
H	0.031460	2.044000	3.064698
H	-1.196363	1.475254	4.190091
C	3.221342	0.817363	3.182565
H	2.423358	1.347973	3.686723
H	3.928404	0.471550	3.932030
H	3.730886	1.514048	2.528090
C	2.052034	-1.429625	3.360884
H	1.613150	-2.253702	2.809177
H	2.832622	-1.826007	4.003954
H	1.293124	-0.993872	3.993208
C	3.854935	-1.141602	1.703354
H	3.487033	-1.990216	1.137898
H	4.421814	-0.506019	1.040300
H	4.531376	-1.507364	2.470799

S2 Min

C	0.120458	-0.027296	-0.086391
C	0.107742	-0.029770	1.354705
C	1.548280	0.011951	1.362438
C	1.545924	0.184065	-0.068400
C	2.549095	0.792846	-1.073516
C	2.624543	-0.413206	2.386218
C	-0.976038	0.268711	2.414685
C	-0.875197	-0.509402	-1.165035
C	3.537939	1.744743	-0.341606
H	4.160541	2.244065	-1.078768
H	2.992674	2.498898	0.214389
H	4.190413	1.218147	0.338274
C	3.358377	-0.290287	-1.841718
H	2.701939	-0.937814	-2.409202
H	4.045930	0.191295	-2.532457
H	3.933411	-0.903869	-1.159740
C	1.806569	1.697146	-2.098460
H	1.151105	1.134581	-2.745879
H	1.222192	2.450181	-1.582091
H	2.539184	2.199552	-2.723941
C	-1.679410	0.659164	-1.802172
H	-1.019193	1.370377	-2.282307
H	-2.361769	0.265100	-2.551084
H	-2.259599	1.185868	-1.055042
C	-1.868860	-1.542515	-0.560948
H	-2.485929	-1.948593	-1.357622
H	-1.327276	-2.358706	-0.096495
H	-2.526434	-1.101869	0.173007
C	-0.124927	-1.283211	-2.286608
H	0.534927	-0.646652	-2.856386
H	0.456052	-2.093506	-1.861072

H	-0.852808	-1.705831	-2.973591
C	-2.124439	1.112670	1.791372
H	-2.817208	1.403083	2.576290
H	-1.726070	2.011863	1.335356
H	-2.681447	0.564771	1.046516
C	-1.574259	-1.023696	3.039235
H	-0.808289	-1.608970	3.532170
H	-2.328341	-0.756477	3.775254
H	-2.039777	-1.642741	2.282719
C	-0.393068	1.160253	3.548225
H	0.357867	0.648273	4.130665
H	0.044420	2.060483	3.131830
H	-1.195860	1.447707	4.221469
C	3.217694	0.793769	3.167007
H	2.447945	1.315357	3.721690
H	3.966583	0.439032	3.870639
H	3.688367	1.499692	2.494415
C	2.033829	-1.435237	3.399196
H	1.599739	-2.278207	2.873685
H	2.831887	-1.802477	4.038415
H	1.278504	-0.997252	4.033953
C	3.777763	-1.175947	1.673535
H	3.383075	-2.013106	1.109103
H	4.339871	-0.542099	1.004556
H	4.464998	-1.559604	2.422453

S1 SP

C	0.076940	-0.066180	-0.136240
C	0.142700	-0.020690	1.320010
C	1.598470	-0.024360	1.407740
C	1.510280	0.182650	-0.033240
C	2.501280	0.826230	-1.026620
C	2.678910	-0.422430	2.438650
C	-0.935340	0.315340	2.372620
C	-0.927650	-0.521690	-1.218770
C	3.513960	1.754980	-0.304120
H	4.146320	2.232040	-1.047550
H	2.991650	2.527380	0.249260
H	4.151550	1.213470	0.377720
C	3.275170	-0.302490	-1.770080
H	2.599660	-0.948580	-2.316230
H	3.965660	0.149010	-2.477420
H	3.843610	-0.910090	-1.077170
C	1.765980	1.717900	-2.062840
H	1.103670	1.146570	-2.695440
H	1.188690	2.485550	-1.559770
H	2.502690	2.201690	-2.697960
C	-1.728530	0.643160	-1.863430
H	-1.064900	1.352880	-2.340900
H	-2.411800	0.255960	-2.615140
H	-2.307990	1.173650	-1.118390
C	-1.930130	-1.548360	-0.618550
H	-2.550570	-1.952080	-1.413920
H	-1.395220	-2.367820	-0.152160
H	-2.587140	-1.102370	0.113690
C	-0.181450	-1.300080	-2.339380
H	0.484880	-0.665410	-2.905410
H	0.392700	-2.114640	-1.912750

H	-0.906520	-1.717240	-3.032780
C	-2.103030	1.131370	1.755640
H	-2.801420	1.397560	2.544010
H	-1.730430	2.044040	1.304150
H	-2.642780	0.571750	1.007210
C	-1.490970	-1.012440	2.967540
H	-0.706700	-1.590410	3.439670
H	-2.242480	-0.777120	3.716410
H	-1.951160	-1.623170	2.200960
C	-0.357140	1.191920	3.515780
H	0.401920	0.674350	4.082530
H	0.070950	2.103590	3.114260
H	-1.160590	1.459310	4.196320
C	3.269510	0.779440	3.226430
H	2.496630	1.299280	3.778260
H	4.018120	0.431230	3.933670
H	3.738820	1.488680	2.556360
C	2.093000	-1.448100	3.450170
H	1.666360	-2.293910	2.923130
H	2.887390	-1.811270	4.096380
H	1.331580	-1.012660	4.080910
C	3.839720	-1.177780	1.730670
H	3.452150	-2.016730	1.164000
H	4.400350	-0.539010	1.064020
H	4.529840	-1.558390	2.478620

S1 TP

C	0.137950	-0.315800	-0.111970
C	0.170700	-0.038820	1.325080
C	1.613540	0.091680	1.440160
C	1.517930	0.161310	-0.008340
C	2.470980	0.848350	-1.010420
C	2.684210	-0.421540	2.444970
C	-0.921270	0.344080	2.347580
C	-0.919300	-0.564350	-1.217550
C	3.469730	1.785600	-0.280360
H	4.098830	2.275270	-1.018310
H	2.936270	2.546350	0.278220
H	4.110690	1.245390	0.399530
C	3.260860	-0.258900	-1.769310
H	2.592890	-0.913330	-2.314800
H	3.937500	0.211440	-2.477940
H	3.845890	-0.861110	-1.085710
C	1.714580	1.734460	-2.034580
H	1.081500	1.151840	-2.686780
H	1.106590	2.472770	-1.523540
H	2.440410	2.256490	-2.651620
C	-1.683200	0.655030	-1.807670
H	-1.007610	1.360860	-2.272740
H	-2.382100	0.309230	-2.564550
H	-2.245640	1.178590	-1.046240
C	-1.961360	-1.573860	-0.654840
H	-2.605790	-1.915500	-1.460480
H	-1.458360	-2.434150	-0.229390
H	-2.590180	-1.131370	0.104500
C	-0.213810	-1.315770	-2.383410
H	0.471530	-0.679180	-2.923980
H	0.334250	-2.169610	-2.002200

H	-0.960220	-1.672570	-3.088250
C	-2.068340	1.170150	1.708710
H	-2.755770	1.479960	2.490250
H	-1.675130	2.059010	1.227320
H	-2.626010	0.598090	0.982980
C	-1.504350	-0.967660	2.951910
H	-0.736880	-1.542980	3.453690
H	-2.271990	-0.712370	3.677870
H	-1.949880	-1.588550	2.184950
C	-0.337200	1.221660	3.486680
H	0.416060	0.698610	4.056460
H	0.101860	2.125760	3.081150
H	-1.139100	1.500240	4.165070
C	3.310290	0.746090	3.254950
H	2.551950	1.272190	3.821200
H	4.055200	0.366790	3.950140
H	3.790270	1.458030	2.595710
C	2.075580	-1.451140	3.438200
H	1.621500	-2.275040	2.898450
H	2.864100	-1.849450	4.070910
H	1.331760	-1.007110	4.084020
C	3.820420	-1.189830	1.712950
H	3.410300	-2.007040	1.130220
H	4.392660	-0.548750	1.057380
H	4.505630	-1.603390	2.447770

CIionic

C	0.212890	-0.526888	-0.068129
C	0.225360	-0.065654	1.327237
C	1.652331	0.099986	1.480195
C	1.524103	0.127819	0.041533
C	2.384869	0.952523	-0.944657
C	2.700133	-0.523072	2.444921
C	-0.871635	0.467224	2.279323
C	-0.855500	-0.739288	-1.178872
C	3.324195	1.912621	-0.169026
H	3.931864	2.467893	-0.878592
H	2.747933	2.616330	0.420437
H	3.987161	1.371436	0.491361
C	3.247026	-0.042131	-1.775853
H	2.625548	-0.745366	-2.315764
H	3.838316	0.518427	-2.495084
H	3.921994	-0.601272	-1.140028
C	1.543513	1.822154	-1.912647
H	1.015544	1.215427	-2.634221
H	0.829809	2.428840	-1.366517
H	2.208393	2.485351	-2.458385
C	-1.625052	0.471752	-1.777115
H	-0.963243	1.173433	-2.262343
H	-2.325380	0.106683	-2.522857
H	-2.189897	1.004832	-1.027091
C	-1.904350	-1.737162	-0.608702
H	-2.552973	-2.080208	-1.410478
H	-1.412091	-2.598609	-0.172235
H	-2.525883	-1.274596	0.146205
C	-0.145915	-1.479270	-2.349210
H	0.536232	-0.827239	-2.878064
H	0.408641	-2.333705	-1.978634

H	-0.888752	-1.832037	-3.059853
C	-1.957726	1.302720	1.555818
H	-2.596626	1.769437	2.299938
H	-1.507265	2.084676	0.954681
H	-2.580524	0.684254	0.925638
C	-1.546226	-0.756390	2.965771
H	-0.833931	-1.312305	3.562522
H	-2.339047	-0.402204	3.619316
H	-1.977906	-1.428894	2.235281
C	-0.246186	1.378207	3.367771
H	0.486233	0.845592	3.958017
H	0.233607	2.238504	2.915642
H	-1.030066	1.726954	4.034830
C	3.404743	0.548517	3.319694
H	2.687390	1.083659	3.929576
H	4.128169	0.074654	3.978852
H	3.926796	1.269753	2.703062
C	2.017660	-1.559113	3.378087
H	1.491327	-2.306570	2.794516
H	2.769984	-2.060006	3.981321
H	1.315750	-1.084695	4.051678
C	3.777954	-1.294780	1.637022
H	3.313020	-2.032923	0.992620
H	4.372590	-0.625661	1.028618
H	4.449682	-1.807888	2.319867

CItetra

C	0.151953	-0.193507	-0.048728
C	0.082836	0.056067	1.434660
C	1.575309	-0.097121	1.423990
C	1.512183	0.354450	-0.011220
C	2.179357	1.531696	-0.741178
C	2.421084	-1.218993	2.060225
C	-0.763507	1.080893	2.217076
C	-0.514559	-1.257997	-0.935563
C	3.233183	2.195854	0.180256
H	3.711490	3.020111	-0.342071
H	2.769647	2.580915	1.081244
H	3.999064	1.483909	0.466407
C	2.889867	0.978739	-2.007840
H	2.170465	0.534272	-2.686970
H	3.400431	1.784488	-2.529402
H	3.621078	0.224103	-1.739057
C	1.136117	2.590781	-1.180162
H	0.365018	2.138624	-1.793717
H	0.665203	3.049023	-0.318635
H	1.623033	3.370457	-1.759770
C	-1.223585	-0.534213	-2.113904
H	-0.503332	-0.000166	-2.724097
H	-1.733877	-1.259571	-2.742703
H	-1.954836	0.176162	-1.743725
C	-1.569558	-2.043375	-0.116499
H	-2.047465	-2.786809	-0.748886
H	-1.107157	-2.550175	0.722692
H	-2.335592	-1.377837	0.265031
C	0.529013	-2.246146	-1.516237
H	1.301027	-1.713383	-2.059973
H	0.998665	-2.819901	-0.726158

H	0.042681	-2.937463	-2.199237
C	-1.893999	1.649235	1.324154
H	-2.501079	2.346248	1.895552
H	-1.483654	2.172141	0.467867
H	-2.537616	0.854325	0.964388
C	-1.397435	0.328521	3.420241
H	-0.625678	-0.070157	4.070168
H	-2.018465	1.006708	4.000365
H	-2.013965	-0.494621	3.075372
C	0.102787	2.243592	2.762308
H	0.917294	1.862887	3.368762
H	0.522165	2.826491	1.951113
H	-0.505452	2.900885	3.377882
C	3.052409	-0.637859	3.356096
H	2.279253	-0.332418	4.053156
H	3.673150	-1.388619	3.839005
H	3.668726	0.225160	3.128144
C	1.554858	-2.445857	2.439786
H	1.137650	-2.912754	1.555677
H	2.162557	-3.180653	2.961033
H	0.738808	-2.152168	3.090905
C	3.553576	-1.659305	1.100046
H	3.145176	-2.060588	0.179610
H	4.197145	-0.822322	0.853415
H	4.160241	-2.427472	1.572004

TS1

0.228063	-0.155195	-0.005456
0.002857	0.053960	1.416485
1.464482	-0.138462	1.268852
1.635062	0.297458	-0.108558
2.344643	1.442765	-0.850870
2.338881	-1.127745	2.071004
-0.879777	0.952206	2.299872
-0.477637	-1.158040	-0.945132
3.518514	1.976897	0.008611
3.993065	2.813341	-0.497703
3.159474	2.316951	0.973802
4.266397	1.209047	0.166961
2.898855	0.934200	-2.208325
2.094347	0.585554	-2.846286
3.417851	1.738448	-2.723997
3.594498	0.116817	-2.053558
1.349140	2.602502	-1.115396
0.504046	2.257523	-1.700213
0.977325	3.007742	-0.182028
1.844430	3.399640	-1.663573
-1.166303	-0.337516	-2.071130
-0.433391	0.213623	-2.649793
-1.698082	-1.007860	-2.741701
-1.877597	0.367329	-1.654026
-1.549968	-1.979587	-0.187368
-2.038708	-2.663269	-0.876479
-1.098613	-2.557793	0.610464
-2.305388	-1.333037	0.241886
0.543111	-2.134945	-1.582407
1.315657	-1.597309	-2.119479
1.014987	-2.744767	-0.820472

0.032111	-2.792000	-2.281077
-2.136338	1.394536	1.507799
-2.738306	2.062742	2.117984
-1.850452	1.918349	0.602243
-2.746937	0.541235	1.237535
-1.325334	0.177674	3.568750
-0.466506	-0.115141	4.162429
-1.965621	0.805728	4.183298
-1.876102	-0.715737	3.295881
-0.089429	2.215106	2.731641
0.808183	1.939915	3.273644
0.198508	2.800363	1.866650
-0.704781	2.835750	3.377692
2.893467	-0.364948	3.306304
2.085386	-0.028429	3.946245
3.537651	-1.021967	3.885243
3.471892	0.499225	2.997515
1.503464	-2.339391	2.557196
1.131537	-2.909845	1.713783
2.125264	-2.990746	3.165541
0.658090	-2.017015	3.153638
3.524758	-1.647049	1.220676
3.167355	-2.178301	0.346255
4.156301	-0.830754	0.892407
4.128959	-2.326824	1.815663

TS2

C	0.270584	-0.352412	0.120240
C	0.066613	-0.013499	1.563192
C	1.593019	-0.044602	1.562341
C	1.391455	0.489773	0.179448
C	2.090289	1.566104	-0.661499
C	2.434950	-1.258349	2.030439
C	-0.776252	1.124340	2.192513
C	-0.426698	-1.302630	-0.862071
C	3.164171	2.274308	0.203420
H	3.651955	3.048084	-0.383679
H	2.716897	2.733218	1.076995
H	3.917487	1.569374	0.535356
C	2.785438	0.896372	-1.879285
H	2.054886	0.445921	-2.541361
H	3.337492	1.645227	-2.441224
H	3.479911	0.129339	-1.555609
C	1.077989	2.617877	-1.186982
H	0.282255	2.143310	-1.748951
H	0.637544	3.175319	-0.369072
H	1.588645	3.318612	-1.841989
C	-1.119861	-0.471530	-1.977228
H	-0.388240	0.065700	-2.569741
H	-1.670873	-1.135821	-2.637852
H	-1.814971	0.243717	-1.552206
C	-1.501962	-2.123045	-0.104715
H	-1.988659	-2.808563	-0.793583
H	-1.056115	-2.697911	0.698114
H	-2.255921	-1.470437	0.319837
C	0.586615	-2.272157	-1.525641
H	1.383245	-1.724831	-2.015570
H	1.025738	-2.936952	-0.791524

H	0.077152	-2.875977	-2.271752
C	-1.870191	1.628780	1.221110
H	-2.483673	2.380199	1.710762
H	-1.429171	2.071677	0.335881
H	-2.515912	0.813842	0.913319
C	-1.463966	0.493011	3.435582
H	-0.720461	0.130757	4.137905
H	-2.082575	1.231738	3.939614
H	-2.091589	-0.341585	3.142436
C	0.093422	2.311764	2.669659
H	0.900212	1.964714	3.306312
H	0.524206	2.841154	1.829156
H	-0.514669	3.010628	3.237510
C	3.120482	-0.804259	3.349755
H	2.375745	-0.542063	4.094003
H	3.738323	-1.605418	3.748326
H	3.748503	0.062676	3.175372
C	1.564607	-2.500056	2.338081
H	1.135311	-2.908633	1.431967
H	2.171817	-3.270518	2.805335
H	0.756699	-2.243871	3.015084
C	3.530593	-1.624370	1.000691
H	3.091126	-1.941119	0.062168
H	4.176740	-0.774893	0.809126
H	4.143332	-2.436121	1.383263

THD

C	0.344801	-0.473235	0.077164
C	0.256920	0.474748	1.206848
C	1.402988	-0.455876	1.143482
C	1.316062	0.637748	0.154038
C	2.119959	1.639639	-0.660053
C	2.354492	-1.308221	1.968665
C	-0.695409	1.206115	2.140094
C	-0.458103	-1.354250	-0.867257
C	3.158262	2.338675	0.254941
H	3.689971	3.103126	-0.306145
H	2.669680	2.810106	1.100085
H	3.880731	1.622310	0.628529
C	2.859208	0.909282	-1.810487
H	2.148936	0.475067	-2.504568
H	3.484546	1.613386	-2.353640
H	3.490322	0.118437	-1.421458
C	1.166571	2.705929	-1.258463
H	0.396057	2.238536	-1.860782
H	0.690074	3.276100	-0.469329
H	1.727651	3.391662	-1.888430
C	-1.196494	-0.473234	-1.907451
H	-0.485704	0.052154	-2.534764
H	-1.821088	-1.096360	-2.542605
H	-1.828231	0.256703	-1.414315
C	-1.497078	-2.172153	-0.057614
H	-2.028206	-2.852490	-0.718643
H	-1.009146	-2.754970	0.715350
H	-2.219965	-1.513779	0.410026
C	0.496083	-2.328380	-1.605251
H	1.266975	-1.782767	-2.137199
H	0.972074	-3.001199	-0.901247

H	-0.064271	-2.921445	-2.323703
C	-1.847673	1.836981	1.316546
H	-2.494470	2.417084	1.970037
H	-1.455848	2.494580	0.548910
H	-2.442817	1.066109	0.840867
C	-1.286874	0.211738	3.171984
H	-0.505310	-0.186099	3.808899
H	-2.016076	0.719376	3.798397
H	-1.779408	-0.614295	2.671820
C	0.070629	2.327097	2.888833
H	0.916108	1.919462	3.430992
H	0.434504	3.071532	2.190056
H	-0.591050	2.815934	3.599549
C	2.945028	-0.464542	3.127495
H	2.162862	-0.157375	3.812070
H	3.673512	-1.053318	3.679291
H	3.438191	0.422020	2.745550
C	1.587781	-2.521059	2.556224
H	1.224496	-3.162764	1.761796
H	2.248826	-3.102692	3.193890
H	0.741838	-2.191374	3.148360
C	3.507502	-1.820533	1.067525
H	3.116381	-2.366940	0.216825
H	4.102971	-0.991856	0.702257
H	4.153812	-2.484586	1.636060

3. IRC calculated by CAS/MixB